Water Research 242 (2023) 120184

Contents lists available at ScienceDirect

Water Research

journal homepage: www.elsevier.com/locate/watres

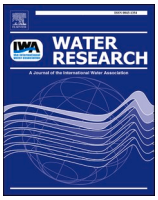

Influence of filter age on Fe, Mn and NH_4^+ removal in dual media rapid sand filters used for drinking water production

Signe Haukelidsaeter [a,*], Alje S. Boersma [b], Liam Kirwan [a], Alessia Corbetta [a], Isaac D. Gorres [b], Wytze K. Lenstra [a], Frank K. Schoonenberg [c], Karl Borger [c], Luuk Vos [d], Paul W.J.J. van der Wielen [d,e], Maartje A.H.J. van Kessel [b], Sebastian Lücker [b], Caroline P. Slomp [a,b]

[a] Department of Earth Sciences, Faculty of Geosciences, Utrecht University, P.O Box 80021, Utrecht 3508 TA, the Netherlands
[b] Department of Microbiology, Faculty of Science, Radboud Institute of Biological and Environmental Science, Radboud University, P.O. Box 9010, Nijmegen 6500 GL, the Netherlands
[c] Vitens N.V., P.O. Box 1205, Zwolle 8001 BE, the Netherlands
[d] KWR Water Research Institute, P.O. Box 1072, Nieuwegein 3430 BB, the Netherlands
[e] Laboratory of Microbiology, Wageningen University & Research, Stippeneng 4, Wageningen 6708 WE, the Netherlands

A B S T R A C T

Rapid sand filtration is a common method for removal of iron (Fe), manganese (Mn) and ammonium (NH_4^+) from anoxic groundwaters used for drinking water production. In this study, we combine geochemical and microbiological data to assess how filter age influences Fe, Mn and NH_4^+ removal in dual media filters, consisting of anthracite overlying quartz sand, that have been in operation for between ~2 months and ~11 years. We show that the depth where dissolved Fe and Mn removal occurs is reflected in the filter medium coatings, with ferrihydrite forming in the anthracite in the top of the filters (< 1 m), while birnessite-type Mn oxides are mostly formed in the sand (> 1 m). Removal of NH_4^+ occurs through nitrification in both the anthracite and sand and is the key driver of oxygen loss. Removal of Fe is independent of filter age and is always efficient (> 97% removal). In contrast, for Mn, the removal efficiency varies with filter age, ranging from 9 to 28% at ~2–3 months after filter replacement to 100% after 8 months. After 11 years, removal reduces to 60–80%. The lack of Mn removal in the youngest filters (at 2–3 months) is likely the result of a relatively low abundance of mineral coatings that adsorb Mn^{2+} and provide surfaces for the establishment of a microbial community. 16S rRNA gene amplicon sequencing shows that *Gallionella,* which are known Fe^{2+} oxidizers, are present after 2 months, yet Fe^{2+} removal is mostly chemical. Efficient NH_4^+ removal (> 90%) establishes within 3 months of operation but leakage occurs upon high NH_4^+loading (> 160 μM). Two-step nitrification by *Nitrosomonas* and *Candidatus* Nitrotoga is likely the most important NH_4^+ removal mechanism in younger filters during ripening (2 months), after which complete ammonia oxidation by *Nitrospira* and canonical two-step nitrification occur simultaneously in older filters. Our results highlight the strong effect of filter age on especially Mn^{2+}but also NH_4^+ removal. We show that ageing of filter medium leads to the development of thick coatings, which we hypothesize leads to preferential flow, and breakthrough of Mn^{2+}. Use of age-specific flow rates may increase the contact time with the filter medium in older filters and improve Mn^{2+} and NH_4^+ removal.

1. Introduction

Groundwater is the main source of drinking water for at least 50% of the global population (Gun, 2012). Unprocessed groundwater often contains undesirable substances such as iron (Fe), manganese (Mn) and ammonium (NH_4^+). These substances can be removed by rapid sand filtration to meet drinking water quality standards (Vries et al., 2017). While Fe usually is successfully removed, incomplete Mn and NH_4^+ removal occurs during the start-up phase of new filters, with efficient Mn removal being achieved only after several weeks to over a year of operation (Tekerlekopoulou et al., 2013). Subsequent ageing of filters can lead to incomplete removal of Mn and NH_4^+, therefore parts of or the complete filter are commonly replaced by new filter medium after a few years of operation (Buamah et al., 2009; Tekerlekopoulou et al., 2013). A better understanding of the processes occurring during ripening and the subsequent ageing phase can help to improve the performance of filters.

In the influent of rapid sand filters, Fe and Mn can be present as either dissolved Fe^{2+} and Mn^{2+} or as particulate Fe and Mn oxides. Dissolved Fe^{2+} and Mn^{2+} can be removed both chemically through homogeneous and/or heterogeneous oxidation and biologically, the latter being generally more important for Mn^{2+} (Bruins et al., 2015c).

* Corresponding author.
E-mail address: s.haukelidsaeter@uu.nl (S. Haukelidsaeter).

https://doi.org/10.1016/j.watres.2023.120184
Received 19 December 2022; Received in revised form 30 April 2023; Accepted 6 June 2023
Available online 10 June 2023

NH_4^+ removal is always biological (Tekerlekopoulou et al., 2013). Homogeneous Fe^{2+} oxidation refers to the process where dissolved Fe^{2+} is oxidized by dissolved oxygen, hydrolyzes, and then precipitates as flocs of Fe-hydroxides (Table 1, Eq. (1); Tamura et al., 1980; Vries et al., 2017). Heterogeneous oxidation consists of a two-step process where Fe^{2+} and/or Mn^{2+} first adsorb to a surface of hydrous ferric oxides (HFOs) or Mn oxides, and then are oxidized and hydrolysed on that surface (Table 1, Eq. (2); Tamura et al., 1980; Vries et al., 2017). Biological oxidation, finally, involves chemolithotrophic microorganisms that utilize Fe^{2+}, Mn^{2+}, or NH_4^+ as electron donors and energy sources for microbial growth, and CO_2 as a carbon source (Table 1, Eqs. (3a), (3b), (3c); Gülay et al., 2014; Mouchet, 1992).

The removal efficiency of Fe^{2+}, Mn^{2+} and NH_4^+ typically depends on the depth in the sand filter (Fig. 1; Table 1). In filters with prior aeration, the supernatant water on top of the filter will be enriched in dissolved oxygen promoting homogeneous oxidation of Fe^{2+} to ferrihydrite. These oxides typically settle on top of the filter as Fe flocs or precipitate between the sand grains on the upper part of the filter medium (de Vet et al., 2009). Homogeneous Mn^{2+} oxidation does not occur in rapid sand filters due to slow oxidation kinetics of Mn^{2+} at pH < 9 (Diem and Stumm, 1984; Vries et al., 2017).

Heterogeneous removal of Fe^{2+} and Mn^{2+} takes place as the water flows through the filter bed (Bruins et al., 2015c; Sharma et al., 1999). Typically, Fe^{2+} is removed at shallower depths than Mn^{2+} due to the faster oxidation kinetics of Fe^{2+} (Vries et al., 2017). With time, heterogeneous Fe^{2+} and Mn^{2+} oxidation results in the development of a coating of ferrihydrite and birnessite-type Mn oxides, respectively (Bruins et al., 2015c; Sharma et al., 2002). Freshly formed coatings act as an adsorbent for Fe^{2+} and Mn^{2+} and further accelerate heterogeneous oxidation as a result of an increased availability of adsorption surfaces (Buamah et al., 2008; Sharma et al., 1999).

The porous mineral coatings also increase the surface area of the filter medium, promoting microbial colonization (Gülay et al., 2014). *Gallionella* and *Leptothrix* are frequently associated with biological Fe^{2+} oxidation in rapid sand filters, yet the contribution of microbes to Fe^{2+} removal can be limited by fast chemical oxidation of Fe^{2+} under fully aerated conditions (Gülay et al., 2018; Van Beek et al., 2016). The conditions favourable for microbial Mn^{2+} oxidation are not fully understood, as many bacteria capable of Fe^{2+} oxidation, can also oxidize Mn^{2+} (Mouchet, 1992). However, *Hyphomicrobium* and *Pseudomonas* have been detected in rapid sand filters and may be involved in Mn^{2+} oxidation (Albers et al., 2015; Bruins et al., 2015c). Biological Mn^{2+} oxidation likely only dominates during the start-up of new filters, before heterogeneous oxidation becomes more important (Bruins et al., 2015a)

Nitrifying microorganisms oxidize NH_4^+ to NO_2^- and subsequently NO_3^- (Van Kessel et al., 2015). This conversion can be performed sequentially by ammonia-oxidizing organisms and nitrite-oxidizing bacteria. However, some species of the genus *Nitrospira* are capable of complete ammonia oxidation to NO_3^- (comammox; Daims et al., 2015; Van Kessel et al., 2015). In rapid sand filters, comammox *Nitrospira* typically outnumber ammonia-oxidizing bacteria such as *Nitrosomonas* and *Nitrosospira* (Fowler et al., 2018; Palomo et al., 2016; Pinto et al., 2016). Nitrification typically depends on the availability of NH_4^+ and O_2 and can be hindered by Fe floc buildup or by copper and phosphate deficiency (de Vet et al., 2012; Wagner et al., 2016). In sand filters receiving high concentrations of NH_4^+ (> 2 mg/l, 110 μM), high nitrification rates can negatively affect Mn^{2+} removal efficiency by decreasing pH and oxygen availability (Gouzinis et al., 1998; Tian et al., 2019). The activity of nitrifying bacteria increases upon the accumulation of metal coatings on sand filters, which is thought to be due to the increase in internal porosity providing a protective layer during backwash (Gülay et al., 2014). Hence, metal coatings not only act as adsorbents in heterogeneous Mn^{2+} oxidation but also provide attachment sites for microorganisms and thereby promote both Mn and NH_4^+ removal (Gülay et al., 2014). Differences in filter performance and microbial community composition are often attributed to differences in groundwater chemistry between drinking water production sites (Albers et al., 2015; Bruins et al., 2015b). We hypothesize that the age and characteristics of the metal coatings and evolution of the microbial community also play a key role in controlling the removal efficiency of Mn and NH_4^+.

In this study, we investigated this hypothesis in four dual media rapid sand filters at a drinking water treatment plant (DWTP) in the Netherlands. Our goal was to assess how filter medium age impacts the processes responsible for the removal of Fe, Mn and NH_4^+, their location within the filters, and their overall efficiency. We used a range of advanced chemical and molecular methods to compare the performance of a newly replaced filter to that of filters that have been in operation for ~1 to ~11 years. Specific attention was given to the temporal evolution of the solute removal efficiency in the sand filters on time scales of months to years, as well as the exact location and mechanism of solute removal within the filter bed. We show that Mn and NH_4^+ removal becomes efficient after 3–5 months of operation, after development of metal oxide coatings and the establishment of a stable microbial community that mediates Fe, Mn and NH_4^+ removal. Old filters fail to completely remove Mn due to changes in coating characteristics, which may change the hydrological properties of the filter, resulting in a lower contact time of the water with the filter medium.

Table 1
Removal processes in rapid sand filters and associated reaction equations (Van Kessel et al., 2015; Vries et al., 2017).

Process	Reaction
1. Homogeneous Fe^{2+} oxidation	$2\ Fe^{2+} + ½\ O_2 + 5\ H_2O \rightarrow 2\ Fe(OH)_3 + 4\ H^+$
2. Heterogeneous Fe^{2+} oxidation	$2\ HFO^*\text{-}\ OH + 2\ Fe^{2+} + ½\ O_2 + 3\ H_2O \rightarrow 2\ HFO - Fe(OH)_3 + 4\ H^+$
3a. Microbial Fe^{2+} oxidation	$2\ Fe^{2+} + ½\ O_2 + 5\ H_2O \rightarrow 2\ Fe(OH)_3 + 4\ H^+$
3b. Microbial Mn^{2+} oxidation	$Mn^{2+} + ½\ O_2 + H_2O + OH \rightarrow\ MnO_2 + 3\ H^+$
3c. Nitrification	$NH_4^+ + 2\ O_2 \rightarrow NO_3^- + 2H^+ + H_2O$

*HFO = hydrous ferric oxides.

2. Materials and methods

2.1. Drinking water treatment plant

At the Vitens DWTP in Sint Jansklooster, in the Netherlands (52°40′41.2″N, 6°00′47.8″E), groundwater is extracted from two main source areas from a total of 18 wells. The source water is characterized by a pH of ~6.9 and a temperature of ~10–11 °C. The combination of groundwater wells in use determines the concentrations of Fe, Mn and NH_4^+ in the inlet water (Table 2). The treatment scheme at the DWTP consists of 11 treatment steps (Supplementary Fig. S1). At first, intense plate aeration removes gases (CH_4, CO_2 and H_2S), then the water is led to the rapid sand filter via cascades. After the rapid sand filtration, the water is treated further, including pellet softening, dosing of CO_2, aeration, a second rapid sand filter and subsequent ion exchange step to remove recalcitrant organic compounds. In this study, we only focused on the first rapid sand filtration step, since that is where most Fe, Mn and NH_4^+ is removed.

The DWTP has 12 parallel 25 m^2 dual media rapid sand filters consisting of 0.9–1 m anthracite (1.4–2.5 mm in diameter; porosity of ~50%) and 1.6 m of sand (0.8–1.2 mm in diameter; porosity of ~42%). The height of the supernatant ranges from ~10–25 cm and the filtration rate from ~45–65 m^3/h depending on the production demand. The feed flow is measured as an average across six parallel filters. Filters are backwashed after approximately 7000 m^3 of water has passed through a filter, on average every 3–4 days. The backwash includes reverse water flow in combination with air to remove flocs that settled on and within the anthracite and sand bed.

The drinking water company (Vitens N.V.) carries out weekly

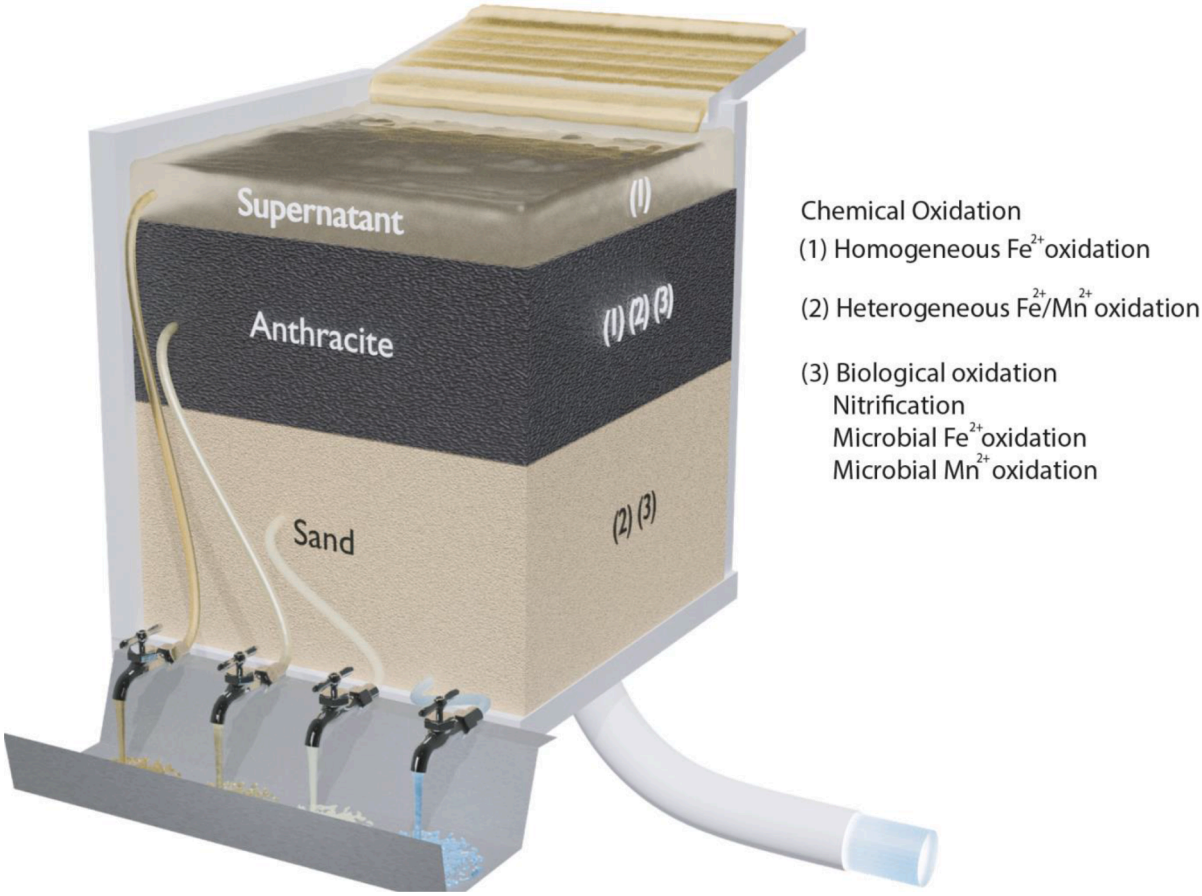

Fig. 1. Schematic of a dual media rapid sand filter with an anthracite and a sand layer. Key removal processes in the filter are as follows: (1) homogeneous Fe^{2+} oxidation, (2) heterogeneous Fe^{2+} and Mn^{2+} oxidation and (3) biological oxidation, which here refers to nitrification and microbial Fe^{2+} and Mn^{2+}oxidation.

measurements of raw water and filter effluent quality. The results from March 2021 to March 2022 were included in this study (Supplementary Method S1).

2.2. Sample collection

Four parallel filters at Sint Jansklooster (prefilters 11, 12, 13 and 14), hereafter referred to as Filters 1, 2, 3 and 4, respectively, were sampled in 2021 and 2022. All four filters had either their anthracite or both anthracite and sand replaced in the 2 years prior to sampling (Table 2; Supplementary Table S1). Water samples were collected in March/April, May and twice in October 2021. For geochemical analysis, filter medium was collected in March/April 2021, and for Filter 3 again in October 2021. Samples for microbial community analysis were collected in March/April 2021, October 2021, and January 2022. Samples for ATP measurements were collected in June 2022. Because of the strong similarities between Filters 1 and 4, all results from Filter 4 are only presented in the supplementary information.

Samples of abstracted groundwater were collected from a tap prior to aeration. Supernatant water samples were collected directly from the top of the filter. To assess Fe, Mn and NH_4^+ removal in the filter, water samples were obtained from 11 taps along the side of Filter 1 (every 20 cm) and 4 taps along Filters 2, 3 and 4 (at depths of 14 cm, 150 cm, 200 cm, and from the filter bottom at 250 cm). Effluent samples were collected from a tap allowing access to water exiting the bottom of each filter.

Oxygen (O_2) concentrations, pH, conductivity, and temperature were measured directly in the water from the taps with a HQ40D Portable Multimeter (HACH), with a tube from each tap leading directly into a 500 ml polypropylene bottle that overflowed continuously. Unfiltered and filtered (< 0.45 μm) water samples were collected in 15 mL tubes and acidified with ultra-pure nitric acid (HNO_3; 10 μL per 1 mL sample) and stored at 4 °C until analysis of Fe and Mn. The Fe and Mn determined in filtered samples was assumed to be a measure of dissolved Fe^{2+} and Mn^{2+}, while Fe and Mn in unfiltered samples additionally include Fe and Mn oxides present as flocs. For the analysis of NH_4^+, NO_2^- and NO_3^-, another filtered sample was collected and stored at −20 °C until analysis.

A stainless-steel peat sampler (Veenlans 04.09, Royal Eijkelkamp, Giesbeek, the Netherlands) was used to collect filter medium samples down to a depth of 2 m in the filter. Samples for geochemical analysis were collected from different depths from the anthracite (16 samples, every 5 cm) and sand (7 samples, every 10 cm) and stored in 50 ml tubes at −20 °C. For analysis of the microbial community, 7 filter medium samples were collected from the anthracite (0–4 cm, 4–10 cm, 10–15 cm, 15–20 cm, 25–30 cm, 30–50 cm, 50–100 cm), and 2 from the sand (100–150 cm, 150–200 cm). Filter medium for DNA isolation were stored at −20 °C and samples for ATP measurements were stored at 4 °C and measured within 24 h.

2.3. Analysis of water chemistry

Particulate and dissolved Fe (Limit of Detection, LOD = 0.023 mg/l) and Mn (LOD = 0.001 mg/l) were analysed using a Perkin-Elmer Avio 500 Inductively Coupled Plasma Optical Emission Spectrophotometer (ICP-OES). The concentration of NH_4^+(LOD = 0.3 μM), NO_2^-(LOD = 0.02 μM) and NO_3^-(LOD = 0.09 μM) in the filtered water samples was determined spectrophotometrically with a Gallery™ Discrete analyzer. NO_x was measured as described in Jumppanen et al. (2014) and NH_4^+ according to ISO7150–1:1984. No data for NO_2^- and

Table 2
Removal of Fe, Mn and NH_4^+. Concentrations of total Fe, Mn, NH_4^+, O_2, and pH in the supernatant (Sn) and effluent (Eff) of Filters 1, 2 and 3, sampled in March/April, May and twice in October 2021. Elevated NH_4^+ (> 120 μM) and Fe (> 499 μM) concentrations in the supernatant are indicated with red shading. Relative removal efficiencies of Fe, Mn, and NH_4^+ in the filters were calculated from the difference in concentration between the supernatant and effluent. Removal efficiencies < 90% are highlighted with red shading.

		Age[a]		Fe		Mn		NH_4^+		O_2			Removal		
Filter	Sampling	A	S	Sn	Eff	Sn	Eff	Sn	Eff	Sn	Eff	$\Delta O_2/\Delta NH_4^+$	Fe	Mn	NH_4^+
				μM	μM	μM	μM	μM	μM	μM	μM		%	%	%
1		2y	11y	136	3.3	5.8	1	62	1	318	112	3.4	97	80	99
2	March/April[b]	7m	7m	154	1.0	7.0	0.07	172	3	315	30	1.7	99	99	98
3		2m	2m	216	1.8	7.8	7	84	10	319	79	3.2	99	9	88
1		2y	11y	525	1.1	8.5	4	128	7	324	30	2.4	100	60	94
2	May	8m	8m	500	3.5	9.1	0.25	143	5	319	30	2.1	99	97	98
3		3m	3m	506	1.2	9.2	7	157	7	313	18	2.0	100	28	96
1		2.5y	11y	134	3.0	6.7	2	162	29	331	52	2.1	98	60	80
2	October (I)	1y	1y	167	4.0	6.5	0.06	161	11	335	52	1.9	98	99	94
3		8m	8m	157	4.3	6.4	0	162	12	338	17	2.1	97	94	93
1		2.5y	11y	121	7.0	6.2	2	81	1	366	164	2.5	99	73	99
2	October (II)	1y	1y	168	3.2	6.7	0.00	83	3	388	160	2.9	98	100	100
3		8m	8m	266	1.3	7.0	0	84	0	369	162	2.5	100	100	100

[a]Age of the anthracite (A) and sand (S); y, years; m, months.
[b]all filters were sampled on different dates.

NO_3^- for the first two samplings are available.

2.4. Geochemical analysis of filter medium

For high resolution imaging and elemental mapping, filter medium was analysed using a Zeiss Evo 15 Scanning electron microscopy with energy dispersive X-ray spectroscopy (SEM-EDS) (Supplementary Method S2). A sequential extraction method was used to characterize the Fe and Mn oxides present in the coatings (Supplementary Method S3). X-ray diffraction (XRD) was performed to determine whether the coatings contained any crystalline Fe or Mn oxides (Supplementary Method S4). Batch adsorption experiments were performed to assess the adsorption characteristics of the filter medium (Supplementary Method S5). Linear adsorption coefficients were estimated from the gradient of the isotherm at an equilibrium concentration of zero. BET surface area analysis was performed to analyse specific surface area (Supplementary Method S6).

2.5. Microbial community analysis

DNA was isolated from the filter medium and used for 16S rRNA gene amplicon sequencing (Method S7), bacterial16S rRNA and archaeal amoA gene qPCR analysis (Supplementary Method S8). In all filters, archaeal amoA copies were close to the detection limit (data not shown) and thus excluded from further analyses. Additionally, ATP measurements were performed as an indicator for microbial activity (Supplementary Method S9).

3. Results

3.1. Water chemistry

The concentrations of Fe, Mn and NH_4^+ in the supernatant varied between samplings, mainly due to changes in the groundwater wells that were used for water extraction (Table 2). Concentrations of Fe in the supernatant reached values of up to 525 μM in May but were only ~130–150 μM at the other sampling times. Manganese was always present at comparatively lower concentrations of 6–9 μM. Concentrations of NH_4^+ in the supernatant varied between 67 and 172 μM. There was substantial oxygen removal in the filters, but the effluent always remained oxygenated (> 18 μM). The pH (~7.3–7.6) and conductivity (~510–560 μSV) decreased with depth in the filters, while temperature was constant at ~11 °C (Supplementary Tables 2–4).

Both particulate and dissolved Fe was present in the supernatant (Fig. 2). Dissolved Fe, which is assumed to be Fe^{2+}, was mostly removed at the top of the anthracite, while particulate Fe was generally removed at depths < 130 cm, with the exception of Filter 3 in May. While there was leakage of primarily particulate Fe from the filters (~1–7 μM), the Fe removal efficiency was always > 97% and did not depend on filter age (Table 2).

Manganese, assumed to be Mn^{2+}, was exclusively present in dissolved form before removal (Fig. 2). Most Mn removal took place in the lower part of the anthracite and the top of the sand with the removal efficiency depending on filter age (Fig. 2; Table 2). In the oldest filter with two-year old anthracite and eleven-year old sand, Mn removal was ~60–80% efficient (Table 2). Similar results were observed for Filter 4 with sand of the same age (Supplementary Table 1). Filter 2 of intermediate age (7 months – 1 year) showed near-complete Mn removal at all times (> 97%). In the youngest filter (Filter 3), only 9% of Mn was removed after two months of operation, but the removal efficiency

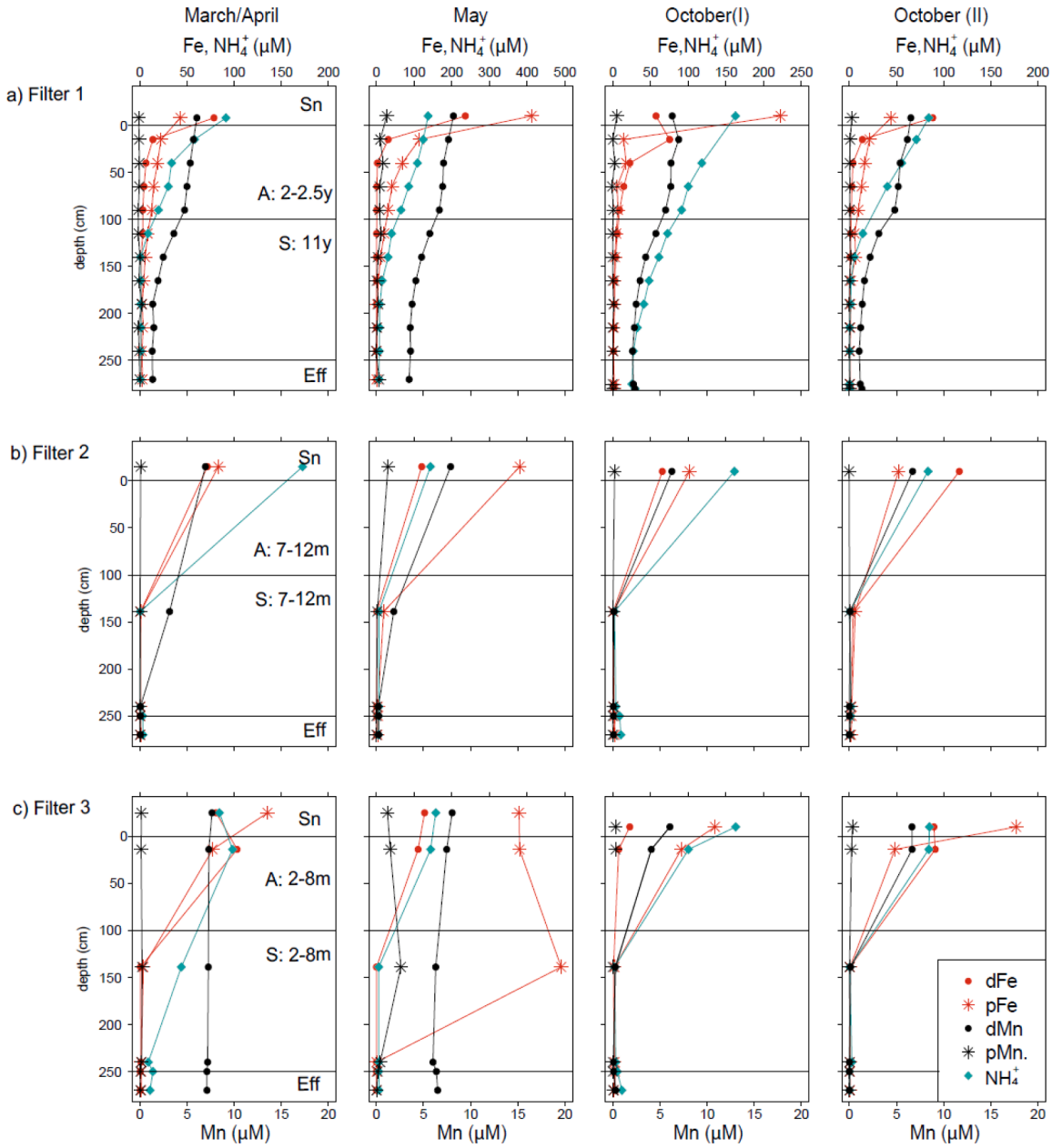

Fig. 2. Removal of Fe, Mn and NH_4^+ with depth in the filter. Dissolved Fe (dFe, red closed circles), particulate Fe (pFe, red stars), dissolved Mn (dMn, black closed circles), particulate Mn (pMn, black stars) and NH_4^+ (light green diamonds) with depth in the filter in (a) Filter 1 (b) Filter 2 and (c) Filter 3 in March/April, May and twice in October 2021 (Filter 4 in Supplementary Fig. S2). Note the different scales for Fe and NH_4^+ in May. The ages of the anthracite (A) and sand (S) are given in the figures. y, year; m, months; Sn, supernatant; Eff, effluent.

increased to 28% after three months, and to > 99% after eight months.

Concentrations of NH_4^+ were highest in May and October (> 150 μM; Table 2). Most of the NH_4^+ was removed in the anthracite; however, when concentrations were > 120 μM, removal also occurred in the sand (Fig. 2). The removal of NH_4^+ was accompanied by a simultaneous increase in NO_3^- indicating nitrification (Supplementary Fig. S3). $NH_4^+$was not always completely removed by all filters and especially in October (I), the oldest filter leaked more NH_4^+ (Filter 1; 29 μM) than the younger ones (Filters 2 and 3; ~12 μM; Table 2). Stochiometric calculations indicate that most O_2 was consumed through nitrification with a $\Delta O_2/\Delta NH_4^+$ ratio close to 2 (Table 2), which is in line with the stoichiometry of the reaction (Table 1).

Trends in effluent concentrations of Fe, Mn and NH_4^+ from March 2021 until March 2022 confirm the impact of filter age on solute leakage. While Fe leakage in all filters was independent of filter age, leakage of Mn and NH_4^+ was more variable, occurring in both the youngest and oldest filter (Fig. 3; Supplementary Fig. S4). Hence, Filter 1 leaked some Mn and NH_4^+, while Filter 2 of intermediate age completely removed these compounds (Supplementary Fig. S4) and Filter 3 achieved complete Mn and NH_4^+ removal only after 150 and 56 days of operation, respectively (Fig. 3). Here, NH_4^+removal established after a transient NO_2^- peak on day 35.

3.2. Filter medium coating

SEM imaging with elemental mapping showed a dense coating (~10 μm) of primarily Fe on the two-year old anthracite of Filter 1 (Fig. 4). The coating on the sand (11 years) consisted of a mixture of Fe and Mn oxides that covered the sand grains. On the anthracite of Filter 2 (7 months), a 1–3 μm thick Fe coating was visible. The equally old sand

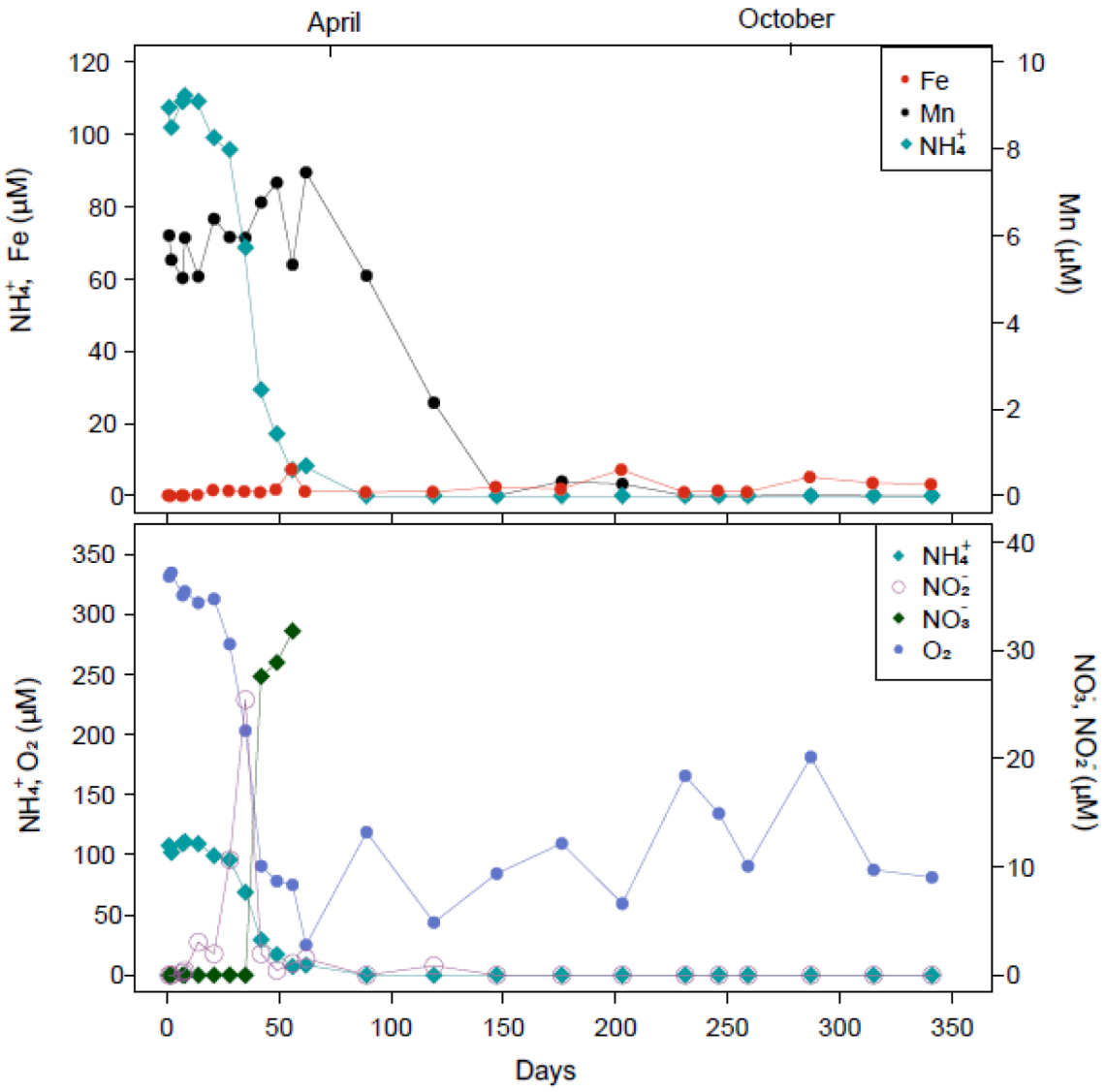

Fig. 3. Temporal change in effluent composition during ripening. Effluent concentrations of NH_4^+ (light green diamonds), Fe (red closed circles), Mn (black closed circles), NO_2^- (purple open cirles), NO_3^- (green closed diamonds) and oxygen (blue closed circles) for Filter 3 during the first year of operation after replacement of the filter material (March 2021-March 2022). Samples were collected and analysed by Vitens N.V. The markings for April and October indicate the approximate times of sampling. Temporal trends for the effluent from other filters are given in Supplementary Fig. S4.

from this filter had a more dispersed, patchy Mn coating compared to Filter 1. Filter 3 (2 months) was characterized by a very thin Fe hydroxide coating on the anthracite and small amounts of Fe hydroxides filled cracks on the sand grains. Manganese was absent from both the anthracite and sand. Twisted stalks and hollow sheets characteristic of Fe-oxidizing bacteria were not detected with SEM imaging.

All the Mn and Fe in the metal coatings was extractable with ascorbic acid and HCl (Table 3), indicating that the Mn and Fe oxides were poorly crystalline, as was also confirmed with XRD (Supplementary Figs. S6 and S7). More Fe was present on the older anthracite of Filter 1 when compared to younger anthracite of Filters 2 and 3, in line with the SEM-EDS results (Fig. 4). The specific surface area of the metal coatings increased with increasing filter age and coating thickness (Table 3).

The Mn^{2+} adsorption experiment revealed that the affinity of the coating for Mn^{2+} increased with filter age and depended on the filter material (Fig. 5). Older coatings adsorbed more Mn^{2+} and there was more adsorption to anthracite than to sand of the same age. Hence, the eleven-year old Mn-coated sand from Filter 1 had the highest affinity for Mn^{2+}, as reflected in the increase of the calculated linear adsorption coefficients with medium type and age (Table 3).

3.3. Microbiology

The two-year old anthracite of Filter 1 was dominated by *Methylomonadaceae* (with an average relative abundance of 30%; Fig. 6A), consisting of members of the genera *Crenothrix* and *Methyloglobulus* (Table 4). Other abundant families include *Nitrospiraceae* (10%), *Gallionellaceae* (8%), *Hyphomicrobiaceae* (6%), *Sphingomonadaceae* (6%) and *Nitrosomonadaceae* (6%). *Gallionella* and *Candidatus* Nitrotoga constituted the dominant genera within the *Gallionellaceae* (Table 4). The same bacterial families were dominant in the seven-month old anthracite of Filter 2, although in different relative abundances. Here, *Gallionellaceae* were most abundant (20%), followed by *Methylomonadaceae* (11%), *Sphingomonadaceae* (9%), *Nitrosomonadaceae* (9%), *Nitrospiraceae* (8%) and *Hyphomicrobiaceae* (3%). In contrast, the two-month old anthracite of Filter 3 was dominated by *Methylomonadaceae* and *Methylophilaceae* (30 and 22%, respectively).

In the eleven-year old sand of Filter 1, *Vicinamibacterales* were most abundant (21%), followed by *Nitrospiraceae* (8%) and *Blastocatellaceae* (6%). In the seven month-old sand of Filter 2, in contrast *Gallionellaceae* were most abundant (10%), followed by *Candidatus* Zambryskibacteria

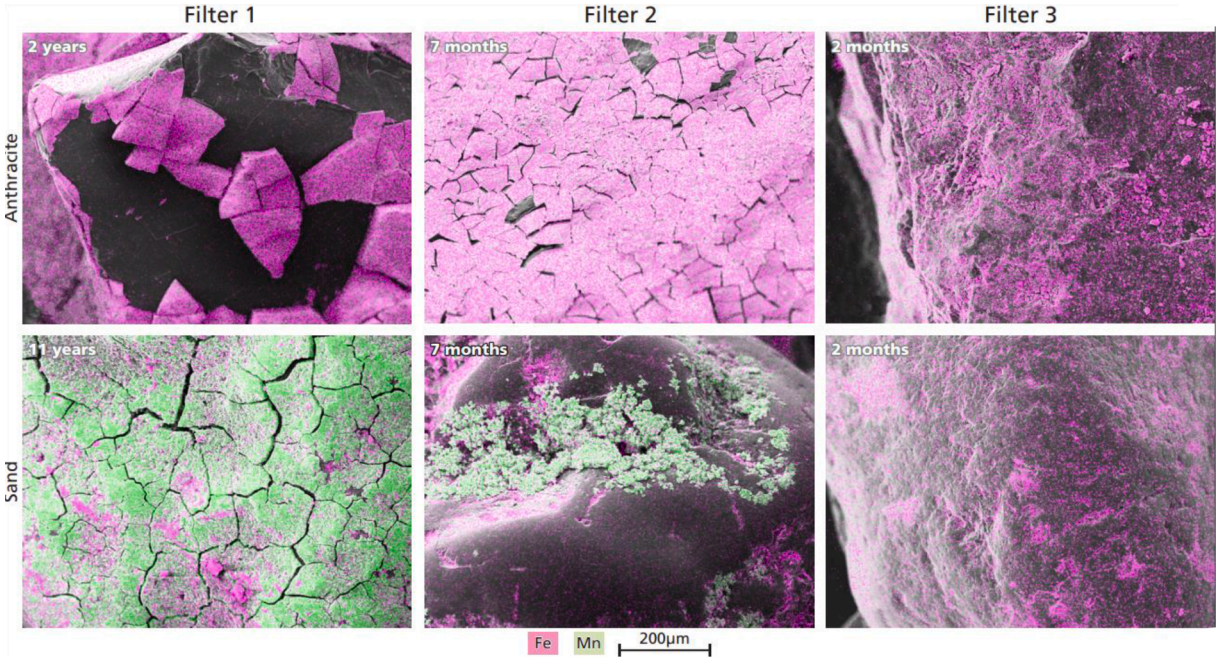

Fig. 4. SEM-EDS images of filter medium coatings. Anthracite (A) and sand (S) particles of Filter 1 (A: 5–10 cm, S: 140–150 cm), Filter 2 (A: 5–10 cm, S: 150–160 cm) and Filter 3 (A: 5–10 cm, S:150–160 cm). Fe is shown in pink, Mn in green. The respective ages of the anthracite and sand are given in the figure, for Filter 4 see Supplementary Fig. S5.

Table 3
Characteristics of the metal coatings. Extracted Fe and Mn from filter grains (µmol/g) and BET-specific surface area of anthracite and sand per volume of material from Filters 1, 2, and 3. The age of the filter material is given in the table (y, years; m, months). The Fe and Mn contents are averages for three depths in the anthracite and sand, respectively. The linear adsorption coefficient K was estimated from the gradient of the adsorption (Fig. 5; supplementary data). n.a., not available.

Filter		Age	Asc Fe (µmol/g)	Asc Mn (µmol/g)	HCl Fe (µmol/g)	HCl Mn (µmol/g)	Surface area (m^2/m^3)	K (l/g)
1	A	2 y	482	29	786	31	6.64×10^6	0.0452
1	S	11 y	139	162	60	112	3.75×10^6	0.0614
2	A	7 m	242	8	17	0	1.68×10^6	0.0401
2	S	7 m	6	19	4	0	1.79×10^5	0.0131
3	A	2 m	43	0	7	0	4.19×10^6	0.0026
3	S	2 m	2	0	4	0	4.11×10^4	0.0159
3	A	8 m	277	11	39	1	1.81×10^6	n.a.
3	S	8 m	6	16	1	1	8.97×10^4	n.a.

(5%), *Candidatus* Kaiserbacteria (4%), *Sphingomonadaceae* (4%) and *Nitrospiraceae* (4%). The sand in Filter 3 after two months of operation was dominated by *Candidatus* Kaiserbacteria (30%) and *Gallionellaceae* (27%). After eight months of operation, the microbial communities of the anthracite and sand of Filter 3 were more similar to those of Filter 2 (Fig. 6B, ANOSIM: $R = 0.4267$, $p = 0.0001$) than after two months (ANOSIM: $R = 0.7987$, $p = 0.0001$). The communities of Filter 3 after eight months still differed from those of the eleven-year old Filter 1 (ANOSIM: $R = 0.5651$, $p = 0.0001$). Thus, the microbial communities of ageing filters continued to change, with filters of similar age having comparable communities (Supplementary Figs. S8 and S9).

Absolute bacterial abundance, based on bacterial 16S rRNA gene copies, was 17 and 30 times higher in the anthracite of Filters 1 and 2, respectively, compared to Filter 3 (Supplementary Fig. S10A). As the anthracite of Filter 3 aged to eight months, the bacterial abundance increased and became the highest of all filters. The microbial abundance in the sand of Filter 3 increased only by a factor of 1.6 within these six months.

ATP concentrations as a measure for microbial activity differed for the anthracite and sand: while ATP concentrations in the anthracite of Filter 3 were higher than in Filter 1, the reverse was observed in the sand (Supplementary Fig. S10B). In both filters, the ATP content in the sand decreased slightly with increasing depth.

4. Discussion

4.1. Mechanisms of Fe, Mn and NH_4^+ removal

In drinking water production, aeration followed by rapid sand filtration is an efficient method for the removal of Fe, Mn and NH_4^+ from groundwater. In our study, we show that all three compounds were successfully removed by a rapid sand filter of intermediate age. However, if the filter was too young or too old, especially Mn removal was not always successful.

Due to plate aeration prior to sand filtration, most Fe entered the filter as particulate Fe flocs formed through homogeneous Fe^{2+} oxidation. As the water flowed through the filter bed, residual Fe^{2+} was removed through heterogeneous and likely also through biological oxidation, since *Gallionella* were present in all Fe^{2+}-removing filters (Fig. 6A). Nevertheless, the characteristic twisted stalks of *Gallionella* were not observed on the filter medium coatings when assessed with SEM imaging. The Fe^{2+} oxidation led to formation of a thick coating of ferrihydrite primarily in the anthracite, as also observed previously (Sharma et al., 1999).

Removal of Mn^{2+} generally only occurred after Fe^{2+} was removed, in line with the slower oxidation kinetics of Mn^{2+} compared to Fe^{2+} (Vries et al., 2017). As a consequence, Mn^{2+} removal was distributed over a

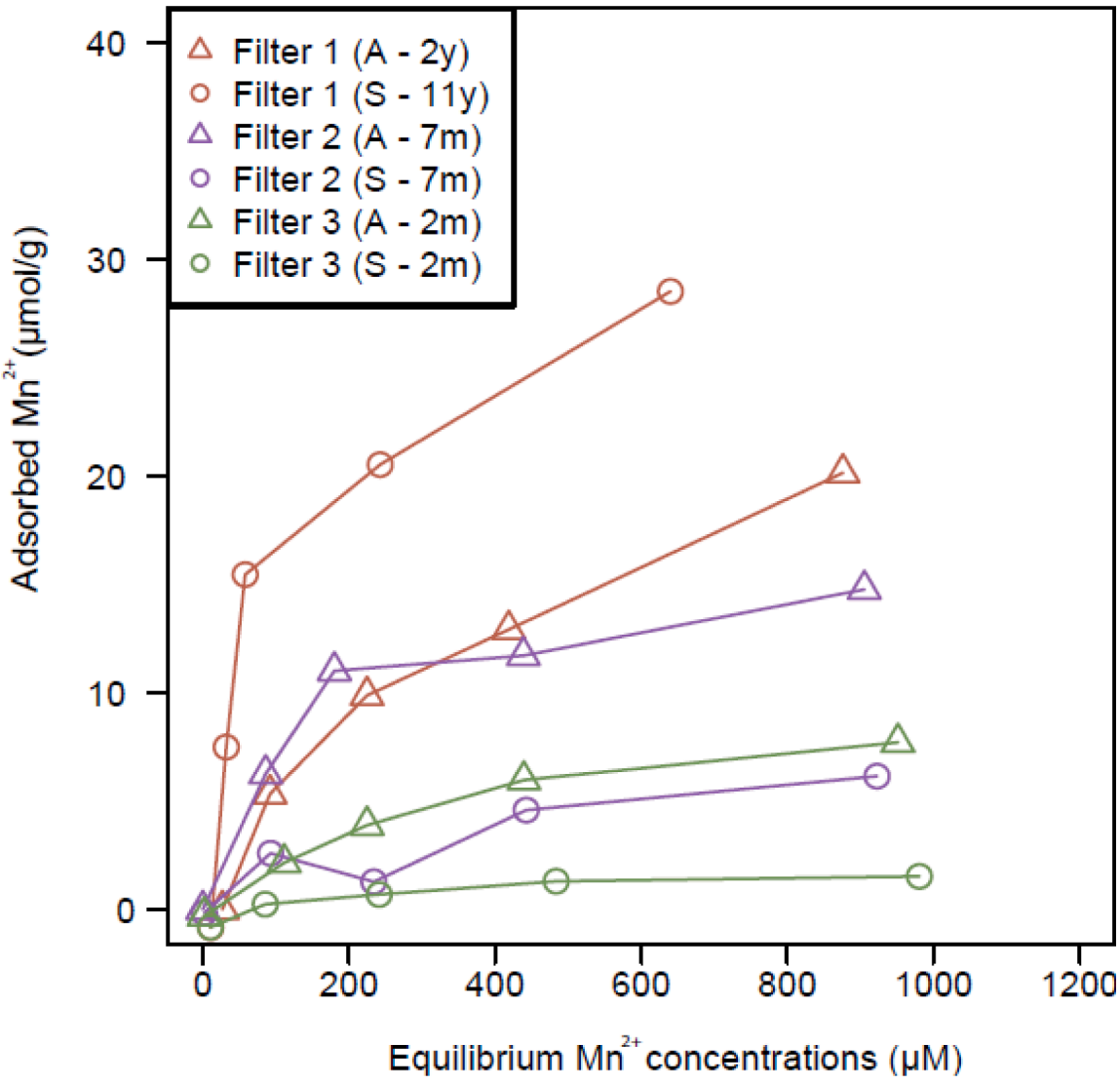

Fig. 5. Adsorption isotherms for Mn^{2+}. Anthracite (triangles) and coated sand (circles) for Filter 1 (red), Filter 2 (purple), and Filter 3 (green). A, anthracite; S, sand; y, years; m, months.

larger depth interval than Fe^{2+} removal. In Filter 1 (anthracite of 2 years and sand of 11 years), Mn^{2+} was mostly removed in the sand; however, in filters of intermediate age (anthracite and sand < 1 year; Filter 2), Mn^{2+} concentrations started to decline already in the anthracite (Fig. 4). Poor Mn^{2+} removal was previously shown to correlate with high Fe loading (> 28 mg/l; > 500 µmol/l; Bruins et al., 2014). Indeed, Mn^{2+} leaked from the oldest filter (Filter 1) in May when Fe^{2+} concentrations reached > 500 µM in the supernatant. Since Mn^{2+} was successfully removed in Filter 2 despite a similar Fe load, the high Fe concentrations alone cannot explain Mn breakthrough.

High concentrations of NH_4^+ may negatively impact Mn^{2+} removal (Gouzinis et al., 1998; Tian et al., 2019). We found that Mn^{2+} removal is indeed less efficient in older filters during high NH_4^+ loading (> 130 µM), although the effect is not observed in the younger filters (Filter 2). The interaction between NH_4^+ and Mn^{2+} removal is typically explained by O_2 depletion and/or an increased H^+ concentrations due to nitrification (Gouzinis et al., 1998; Tian et al., 2019). While low oxygen will limit Mn^{2+}oxidation, the lower pH is expected to negatively affect Mn^{2+} adsorption. However, we find a similar decrease in O_2 and pH with depth in all filters (Supplementary Fig. S3; Supplementary Tables S2–S4), indicating that these parameters alone cannot explain the reduced Mn^{2+} removal efficiency in the presence of elevated NH_4^+ concentrations.

In the older Filter 1, *Nitrospira* were the most abundant nitrifiers indicating complete NH_4^+ oxidation, as has been described for rapid sand filtration previously (Fowler et al., 2018; Gülay et al., 2016; Tatari et al., 2017). In Filter 2 (7 months old) and Filter 3 (8 months old), however, *Nitrospira* and *Nitrosomonas* were equally abundant, suggesting that canonical two-step nitrification dominates in young filters, which was further supported by the presence of *Candidatus* Nitrotoga. Archaeal ammonia-oxidizers were virtually absent and thus did not contribute to nitrification in these filters. Nitrifiers were most abundant in the anthracite, which is in line with the observed higher NH_4^+ removal in the top of the filter and, thus, higher nitrification rates in the anthracite compared to the sand. Nitrification can be hindered by the buildup of Fe flocs in the upper part of rapid sand filters (de Vet et al., 2009) but high Fe loads (~500 µM; 28 mg/l; May sampling) still allowed near-complete NH_4^+ removal in the investigated DWTP (Table 2), suggesting that backwash intervals were frequent enough.

5. Ripening of filter medium

At the Sint Jansklooster DWTP, the replacement of Filter 3 led to leakage of both Mn^{2+} and NH_4^+, whereas Fe was efficiently removed

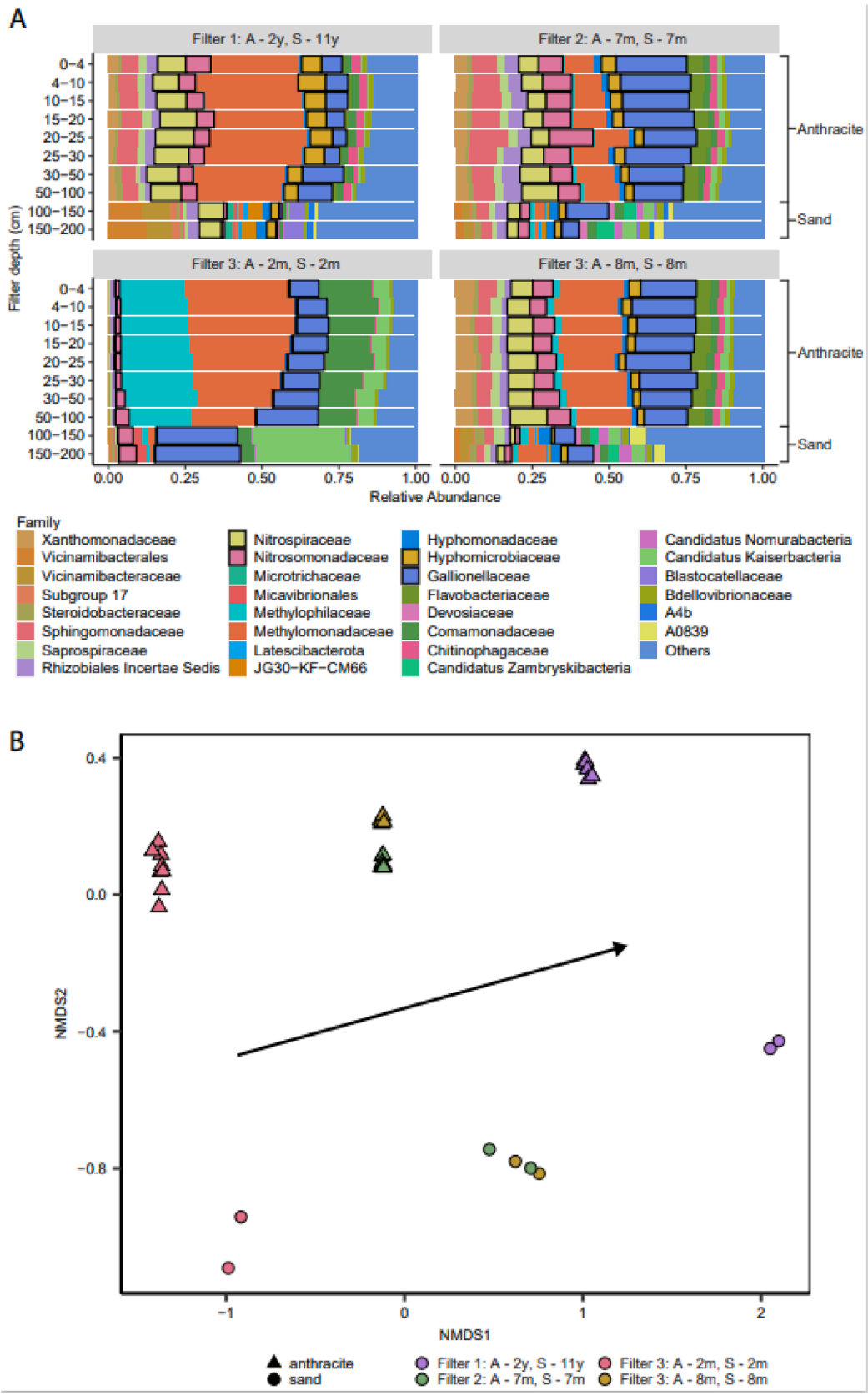

Fig. 6. Microbial community composition. 16S rRNA gene amplicon sequencing-based relative microbial abundances (A) and non-metrical multidimensional scaling plot (B) of Filters 1, 2, and 3. One sampling time point is shown for Filters 1 and 2, two for Filter 3. A: *Nitrospiraceae, Nitrosomonadaceae, Hyphomicrobiaceae* and *Gallionellaceae* are highlighted. B: The arrow indicates the change in ordination space as the filter age increases. The relative microbial communities and NMDS plot including Filter 4 and one additional time point for all four filters are included in Supplementary Figs. S8 and S9, respectively. The respective ages of the anthracite and sand are shown in the figure legend.

Table 4
Abundance of main genera in most abundant families. The table indicates the genera that constitute the most abundant families of Filters 1–3. The age of the filter material is given in the table (A, anthracite; S, sand; y, years; m, months).

Family	Genus	Filter 1 A (2 y)	Filter 1 S (11 y)	Filter 2 A (7 m)	Filter 2 S (7 m)	Filter 3 A (2 m)	Filter 3 S (2 m)	Filter 3 A (8 m)	Filter 3 S (8 m)
Methylomonadaceae	*Methyloglobulus*	82%	85%	26%	18%	1%	1%	25%	25%
	Crenothrix	16%	14%	55%	67%	86%	91%	67%	67%
Nitrospiraceae	*Nitrospira*	100%	100%	100%	100%	100%	100%	100%	100%
Nitrosomonadaceae	*Nitrosomonas*	100%	100%	100%	100%	100%	100%	100%	100%
Gallionellaceae	*Gallionella*	79%	96%	27%	57%	34%	13%	54%	57%
	Candidatus Nitrotoga	20%	4%	62%	38%	64%	87%	44%	43%
Hyphomicrobiaceae	*Hyphomicrobiaceae*	87%	37%	89%	75%	92%	83%	92%	77%
	Pedomicrobium	8%	38%	8%	18%	7%	17%	7%	19%
Sphingomonadaceae	*Novosphingobium*	68%	80%	23%	40%	12%	38%	31%	34%
	Spingorhabdus	17%	2%	67%	28%	66%	33%	40%	14%

directly (Fig. 3). Successful removal of NH_4^+ and Mn^{2+} was achieved after 56 days and 150 days of operation, respectively (Table 2; Fig. 3). This is in line with earlier work demonstrating the necessity of filter medium ripening for Mn^{2+} and NH_4^+ removal (Buamah et al., 2009; Tekerlekopoulou et al., 2013). For Mn^{2+}, ripening is thought to involve an initial phase of biological oxidation and, subsequently, heterogeneous oxidation, which requires adsorption of Mn^{2+} on metal oxides (Breda et al., 2019; Bruins et al., 2015a).

We show that two months after filter replacement, when only 9% of the incoming Mn was removed in Filter 3, both the anthracite and sand were largely devoid of Mn oxides (Table 2; Fig. 4; Supplementary Fig. S6). This explains the limited adsorption of Mn^{2+} to the filter material (Fig. 5; Bruins et al., 2015c). The dominance of *Methylophilaceae* and *Methylomonadaceae* indicates that some methane (CH_4) entered the filter after plate aeration and was removed by methane-oxidizing bacteria in the top of the filter. The presence of *Nitrosomonas* and *Candidatus* Nitrotoga suggest that two-step nitrification dominated during ripening, resulting in 80% NH_4^+ removal.

Seven and eight months after filter replacement, a thin coating of Fe hydroxides had established on the anthracite, whereas patches of Mn oxides had developed primarily in irregularities on the sand in Filters 2 and 3 (Fig. 4). By this time, Mn^{2+} and NH_4^+ removal in the filter was near complete, with an efficiency of $\geq$ 97% and 98%, respectively, and the microbial community in Filter 3 had become similar to that of Filter 2 (7 months; Fig. 6A). Additionally, the total bacterial abundance had increased in the anthracite and, to a lesser extent, in the sand (Supplementary Fig. S10A), confirming earlier observations that microbial abundance increases with coating thickness (Gülay et al., 2014).

Our results for Filters 2 and 3 show efficient Mn removal in young filters, where Mn coatings were limited (Figs. 4, 5). Both *Hyphomicrobium* and *Pedomicrobium* were present in all filters and have linked to Mn^{2+} oxidation in rapid sand filters (Albers et al., 2015; Larsen et al., 1999; Palermo and Dittrich, 2016). This could fit with a scenario where Mn^{2+} oxidation starts biological before proceeding as a combination of biological and heterogeneous oxidation, as suggested in previous work (Bruins et al., 2015c).

6. Ageing effect on coating characteristics and microbial community

Ageing of rapid sand filters may lead to leakage of Mn^{2+} and to some extent NH_4^+ (Tekerlekopoulou et al., 2013). We observed that Filter 1 (two- and eleven-year old anthracite and sand, respectively), had a substantially lower Mn^{2+} and NH_4^+ removal efficiency (60 *vs.* 99% for Mn^{2+}, and 80 *vs.* 94% for NH_4^+ in October (I); Table 2) when compared to the younger filters. We identified three possible factors linked to Mn^{2+} and NH_4^+ removal that may change with the age of the filter medium. These are (1) the characteristics of the metal oxide coatings (2) the abundance, composition, and activity of the microbial community in the filter and (3) the contact time of the water with the sand filter. Below, we discuss the role of each of these factors in the rapid sand filters at the Sint Jansklooster DWTP.

Our SEM-EDS and extraction results showed that ageing results in a thickening of the Fe and Mn oxide coatings. Most Fe was deposited on the anthracite, while Mn mainly accumulated on the sand particles, and consisted of ferrihydrite and birnessite-type Mn oxides, respectively (Table 3; Supplementary Figs. S7 and S8). We showed that older coatings (Filter 1) have an almost 100 times larger specific surface area when compared to newly replaced sand (Filter 3), which can be attributed to the large surface area of the Mn oxide coatings (Table 3). The older filters also have a greater potential for Mn^{2+} adsorption (Fig. 5). It could be hypothesized that the increased Fe hydroxides in older coatings, as observed in Filter 1, could hinder Mn^{2+} adsorption on the Mn oxides (Buamah et al., 2008). This is, however, not supported by the results of the adsorption experiments, since the oldest sand (11 years) had the highest affinity for Mn^{2+} (Fig. 5). The higher surface area and thickness of the coatings were furthermore expected to promote nitrification by providing more room for attachment of microorganisms (Gülay et al., 2014). Indeed, a slightly higher relative abundance of *Nitrospira* was detected on the older coated sand compared to the younger, less coated filter medium (Fig. 6; Table 2). Yet, the leakage of NH_4^+ from old filters suggests that other factors than metal coatings account for successful removal of NH_4^+.

The microbial communities of Filters 2 and 3 (7 and 8 months old, respectively) were highly similar. This indicates that with the same inlet water as inoculum and under the same selective pressures arising from the groundwater chemistry, filters of a similar age develop towards a similar microbial community structure (Supplementary Fig. S9). Yet, the evolution of the microbial community continues as the filters become older (here, Filter 1 and 4), with an increased abundance of methanotrophs compared to *Gallionella* and *Hyphomicrobiaceae* (Fig. 6). The higher NH_4^+ removal efficiency in the anthracite of younger filters might be explained by a higher absolute abundance of total bacteria and higher microbial activity in younger filters (Supplementary Fig. S10).

We hypothesize that the water flow through the filter changed as a result of increased grain size, related to the presence of thicker coatings. As a consequence, preferential flow, is expected to have occurred in the older filters, leading to a lower contact time of the water with the filter medium, thereby explaining the lower removal efficiency for Mn and NH_4^+.

7. Implications for drinking water treatment

Drinking water production at the Sint Jansklooster DWTP includes several additional treatment processes after the rapid sand filtration step investigated in this study. Together, the treatment processes are effective in removing Fe, Mn and NH_4^+ to meet drinking water standards. Hence, a slow ripening process of new filters has no negative implications for the quality of the produced drinking water at this plant. However, successful Mn and NH_4^+ removal in prefilters remains of great

benefit to drinking water companies because it reduces clogging of pipes and distribution systems within treatment plants. Also, at some DWTPs, aeration and rapid sand filtration are the only treatment steps. In such cases, there will be Mn leakage into the final drinking water during the ripening of a new filter. A reduction of ripening time of newly started filters therefore remains of high interest.

Since the microbial community and metal oxide coatings together contribute to Mn and NH_4^+ removal, a reduction of the ripening time can be achieved if new filter medium is mixed with that of an active filter (Bruins et al., 2015b; Breda et al., 2019). Secondary rapid sand filters showed Mn removal immediately when inoculated with anthracite from an active filter (Bruins et al., 2015c). In pilot filters, Mn removal was even observed from day 1 when 20% sand from an active filter was added (Breda et al., 2019). However, at the Sint Jansklooster DWTP, inoculating new filters with ripened anthracite will likely not improve initial Mn removal significantly, as most of the Mn is removed in the sand. Rather, our data indicate that to minimize ripening times, the sand should be inoculated with sand from an old filter with metal coatings that allow adsorption of Mn^{2+} and a microbial community that can mediate Mn^{2+} and NH_4^+ removal. In dual media filters, the sand cannot be changed without removing the overlying anthracite. Therefore, to achieve optimal Mn removal after filter bed replacement, it might prove beneficial to retain and reuse up to 20% of the old sand from the filter instead of replacing it completely. A previous study using pilot filters highlighted the importance of keeping this reused coated sand moist, as it lost the heterogeneous adsorption capacity and microbial activity after drying out (Bruins et al., 2015b). However, verification of the efficiency of the proposed replacement strategy in a full-scale dual rapid sand filter is required.

Based on the hypothesis that preferential flow of the water in older filters impacts Mn^{2+} and NH_4^+ removal, we recommend regulating the water flow of each filter individually rather than averaging across an entire line of filters, as is done in the treatment plant investigated. Reducing the water flow rates in older filters allows a longer contact time of the water with the older filter medium. This likely will improve Mn^{2+} and NH_4^+ removal, resulting in longer operating times of rapid sand filters.

8. Conclusions

In this study we show that filter medium age strongly affects Mn and NH_4^+ removal, while Fe removal is not impacted. By comparing rapid sand filters of different ages and following the development in solute removal in a new filter over time, we show that a ripening time of several months is needed to remove Mn and NH_4^+ efficiently. This allows the development of metal oxide coatings and a microbial community that both contribute to removal of Mn and NH_4^+.

Ripened filters were characterized by thin Fe-coated anthracite and Mn-coated sand and achieved complete Mn removal, even upon high Fe and NH_4^+ concentrations in the inlet water. After ripening, all filters developed similar microbial communities, with *Methylomonadaceae, Gallionellaceae, Nitrospiraceae, Nitrosomonadaceae, Sphingomonadaceae,* and *Hyphomicrobiaceae* as the most abundant microorganisms. Diverse, mainly canonical nitrifiers were present in the younger filters (2 months), while *Nitrospira* additionally became abundant in older filters. Nitrification in the older filters presumably took place as both two-step nitrification and complete ammonia oxidation performed by comammox *Nitrospira*. To obtain a better understanding of the potential capability of the detected microorganisms to oxidize Fe^{2+} and Mn^{2+}, and to discern canonical and comammox Nitrospira, we recommend performing metagenomic analyses of ageing filters.

Ageing of sand filters leads to lower Mn removal efficiencies despite the development of a thicker coating with an increased surface area and a greater Mn^{2+} adsorption potential. Similarly, more NH_4^+ leaks from older filters, despite the high abundance of nitrifying bacteria and increase in attachment surfaces provided by thicker coatings. We attribute the deterioration in Mn and NH_4^+ removal efficiency to preferential water flow in older filters and a reduction in the contact time of the water with the filter medium. Future studies should further investigate how the hydraulic properties of the filters change in relation to coating development upon ageing.

Declaration of Competing Interest

The authors declare that they have no known competing financial interests or personal relationships that could have appeared to influence the work reported in this paper.

Data Availability

I share all the data with my paper.

Acknowledgements

We are grateful to H. Doeve, M. Pipping and Vitens N.V. for their support and collaboration during the visits to the drinking water plants. We also thank L. Piso, N.A.G.M. van Helmond, J. Visser, E. Hellebrand and J.J. Mulder, A. Leeuwen-Tolboom, K. Pelsma and P. Kragt for analytical support, and T. Marcus for graphical design. This research was funded by the Netherlands Organisation for Scientific Research (NWO) partnership program Dunea–Vitens: Sand Filtration (grant 17841). MAHJvK and SL were funded by NWO (016.Veni.192.062 and 016.Vidi.189.050, respectively), CPS by the European Research Council (ERC Synergy Grant 694407 MARIX).

Supplementary materials

Supplementary material associated with this article can be found, in the online version, at doi:10.1016/j.watres.2023.120184.

References

Albers, C.N., Ellegaard-Jensen, L., Harder, C.B., Rosendahl, S., Knudsen, B.E., Ekelund, F., Aamand, J., 2015. Groundwater chemistry determines the prokaryotic community structure of waterworks sand filters. Environ. Sci. Technol. 49 (2), 839–846. https://doi.org/10.1021/es5046452.

Breda, I.L., Søborg, D.A., Ramsay, L., Roslev, P., 2019. Manganese removal processes during start-up of inoculated and non-inoculated drinking water biofilters. Water Qual. Res. J. 54 (1), 47–56. https://doi.org/10.2166/wqrj.2018.016.

Bruins, J.H., Petrusevski, B., Slokar, Y.M., Huysman, K., Joris, K., Kruithof, J.C., Kennedy, M.D., 2015a. Biological and physico-chemical formation of Birnessite during the ripening of manganese removal filters. Water Res. 69 (0), 154–161. https://doi.org/10.1016/j.watres.2014.11.019.

Bruins, J.H., Petrusevski, B., Slokar, Y.M., Huysman, K., Joris, K., Kruithof, J.C., Kennedy, M.D., 2015b. Reduction of ripening time of full-scale manganese removal filters with manganese oxide-coated media. J. Water Supply Res. Technol. AQUA 64 (4), 434–441. https://doi.org/10.2166/aqua.2015.117.

Bruins, J.H., Petrusevski, B., Slokar, Y.M., Kruithof, J.C., Kennedy, M.D., 2015c. Manganese removal from groundwater: characterization of filter media coating. Desalin. Water Treat. 55 (7), 1851–1863. https://doi.org/10.1080/19443994.2014.927802.

Bruins, J.H., Vries, D., Petrusevski, B., Slokar, Y.M., Kennedy, M.D., 2014. Assessment of manganese removal from over 100 groundwater treatment plants. J. Water Supply Res. Technol. AQUA 63 (4), 268–280. https://doi.org/10.2166/aqua.2013.086.

Buamah, R., Petrusevski, B., de Ridder, D., van de Wetering, T.S.C.M., Shippers, J.C., 2009. Manganese removal in groundwater treatment: practice, problems and probable solutions. Water Sci. Technol. Water Supply 9 (1), 89–98. https://doi.org/10.2166/ws.2009.009.

Buamah, R., Petrusevski, B., Schippers, J.C., 2008. Adsorptive removal of manganese(II) from the aqueous phase using iron oxide coated sand. J. Water Supply Res. Technol. AQUA 57 (1), 1–11. https://doi.org/10.2166/aqua.2008.078.

Daims, H., Lebedeva, E.V., Pjevac, P., Han, P., Herbold, C., Albertsen, M., Jehmlich, N., Palatinszky, M., Vierheilig, J., Bulaev, A., Kirkegaard, R.H., Von Bergen, M., Rattei, T., Bendinger, B., Nielsen, H., & Wagner, M. (2015). Complete nitrification by Nitrospira bacteria Enrichment of conspicuous Nitrospira. 10.1038/nature16461.

de Vet, W.W.J.M., Rietveld, L.C., Van Loosdrecht, M.C.M., 2009. Influence of iron on nitrification in full-scale drinking water trickling filters. J. Water Supply Res. Technol. AQUA 58 (4), 247–256. https://doi.org/10.2166/aqua.2009.115.

de Vet, W.W.J.M., Van Loosdrecht, M.C.M., Rietveld, L.C., 2012. Phosphorus limitation in nitrifying groundwater filters. Water Res. 46 (4), 1061–1069. https://doi.org/10.1016/j.watres.2011.11.075.

Diem, D., Stumm, W., 1984. Is dissolved Mn2+ being oxidized by O2 in absence of Mn-bacteria or surface catalysts? Geochim. Cosmochim. Acta 48 (7), 1571–1573. https://doi.org/10.1016/0016-7037(84)90413-7.

Fowler, S.J., Palomo, A., Dechesne, A., Mines, P.D., Smets, B.F., 2018. Comammox Nitrospira are abundant ammonia oxidizers in diverse groundwater-fed rapid sand filter communities. Environ. Microbiol. 20 (3), 1002–1015. https://doi.org/10.1111/1462-2920.14033.

Gouzinis, A., Kosmidis, N., Vayenas, D.V., Lyberatos, G., 1998. Removal of Mn and simultaneous removal of NH3, Fe and Mn from potable water using a trickling filter. Water Res. 32 (8), 2442–2450. https://doi.org/10.1016/S0043-1354(97)00471-5.

Gülay, A., Çekiç, Y., Musovic, S., Albrechtsen, H.J., Smets, B.F., 2018. Diversity of iron oxidizers in groundwater-fed rapid sand filters: evidence of Fe(II)-dependent growth by curvibacter and undibacterium spp. Front. Microbiol. 9, 1–14. https://doi.org/10.3389/fmicb.2018.02808. December.

Gülay, A., Musovic, S., Albrechtsen, H.J., Al-Soud, W.A., Sørensen, S.J., Smets, B.F., 2016. Ecological patterns, diversity and core taxa of microbial communities in groundwater-fed rapid gravity filters. ISME J. 10 (9), 2209–2222. https://doi.org/10.1038/ismej.2016.16.

Gülay, A., Tatari, K., Musovic, S., Mateiu, R.V., Albrechtsen, H.J., Smets, B.F., 2014. Internal porosity of mineral coating supports microbial activity in rapid sand filters for groundwater treatment. Appl. Environ. Microbiol. 80 (22), 7010–7020. https://doi.org/10.1128/AEM.01959-14.

van der Gun, J., 2012. Groundwater and Global change: Trends, Opportunities and Challanges. United Nations Educational, Scientific and Cultural Organization.

Jumppanen, T., Jokinen, M., Airo, J., Klemm, M., Hoger, D., Suoniemi-Kähärä1, A., 2014. Automated Total Oxidized Nitrogen Method Using Vanadium as Reductant with Correlation to Cadmium and Hydrazine Reductant Methods in Sea, Natural, and Waste Waters. Thermo Fisher Scientific.

Larsen, E.I., Sly, L., & McEwan, A.G. (1999). Manganese(II) adsorption and oxidation by whole cells and a membrane fraction of Pedomicrobium sp. ACM 3067.

Mouchet, P., 1992. From conventional to biological removal of iron and manganese in France. J. Am. Water Works Assoc. 84 (4), 158–167. https://doi.org/10.1002/j.1551-8833.1992.tb07342.x.

Palermo, C., Dittrich, M., 2016. Evidence for the biogenic origin of manganese-enriched layers in Lake Superior sediments. Environ. Microbiol. Rep. 8 (2), 179–186. https://doi.org/10.1111/1758-2229.12364.

Palomo, A., Jane Fowler, S., Gülay, A., Rasmussen, S., Sicheritz-Ponten, T., Smets, B.F., 2016. Metagenomic analysis of rapid gravity sand filter microbial communities suggests novel physiology of Nitrospira spp. ISME J. 10 (11), 2569–2581. https://doi.org/10.1038/ismej.2016.63.

Pinto, A.J., Marcus, D.N., Ijaz, U.Z., Bautista-de lose Santos, Q.M., Dick, G.J., Raskin, L., 2016. Metagenomic evidence for the presence of comammox nitrospira -like bacteria in a drinking water system. mSphere 1 (1). https://doi.org/10.1128/MSPHERE.00054-15/SUPPL_FILE/SPH001160049SF4.PDF.

Sharma, S., Petrusevski, B., Schippers, J.C., 2002. Characterisation of coated sand from iron removal plants. Water Sci. Technol. Water Supply 2 (2), 247–257. https://doi.org/10.2166/ws.2002.0070.

Sharma, S.K., Greetham, M.R., Schippers, J.C., 1999. Adsorption of iron(ii) onto filter media. J. Water Supply Res. Technol. AQUA 48 (3), 84–91. https://doi.org/10.2166/aqua.1999.0009.

Tamura, H., Kawamura, S., Hagayama, M., 1980. Acceleration of the oxidation of Fe^{2+} ions by Fe(III)-oxyhydroxides. Corros. Sci. 20 (8–9), 963–971. https://doi.org/10.1016/0010-938X(80)90077-3.

Tatari, K., Musovic, S., Gülay, A., Dechesne, A., Albrechtsen, H.J., & Smets, B.F. (2017). Density and distribution of nitrifying guilds in rapid sand filters for drinking water production: Dominance of Nitrospira spp. 10.1016/j.watres.2017.10.023.

Tekerlekopoulou, A.G., Pavlou, S., Vayenas, D.V., 2013. Removal of ammonium, iron and manganese from potable water in biofiltration units: a review. J. Chem. Technol. Biotechnol. 88 (5), 751–773. https://doi.org/10.1002/jctb.4031.

Tian, X., Zhang, R., Huang, T., Wen, G., 2019. The simultaneous removal of ammonium and manganese from surface water by MeOx: side effect of ammonium presence on manganese removal. J. Environ. Sci. (China) 77, 346–353. https://doi.org/10.1016/j.jes.2018.09.006.

Van Beek, C.G.E.M., Dusseldorp, J., Joris, K., Huysman, K., Leijssen, H., Schoonenberg Kegel, F., De Vet, W.W.J.M., Van De Wetering, S., Hofs, B., 2016. Contributions of homogeneous, heterogeneous and biological iron(II) oxidation in aeration and rapid sand filtration (RSF) in field sites. J. Water Supply Res. Technol. AQUA 65 (3), 195–207. https://doi.org/10.2166/aqua.2015.059.

Van Kessel, M.A.H.J., Speth, D.R., Albertsen, M., Nielsen, P.H., Op Den Camp, H.J.M., Kartal, B., Jetten, M.S.M., Lücker, S., 2015. Complete nitrification by a single microorganism. Nature 528 (7583), 555–559. https://doi.org/10.1038/nature16459.

Vries, D., Bertelkamp, C., Schoonenberg Kegel, F., Hofs, B., Dusseldorp, J., Bruins, J.H., de Vet, W., van den Akker, B., 2017. Iron and manganese removal: recent advances in modelling treatment efficiency by rapid sand filtration. Water Res. 109, 35–45. https://doi.org/10.1016/j.watres.2016.11.032.

Wagner, F.B., Nielsen, P.B., Boe-Hansen, R., Albrechtsen, H.J., 2016. Copper deficiency can limit nitrification in biological rapid sand filters for drinking water production. Water Res. 95, 280–288. https://doi.org/10.1016/j.watres.2016.03.025.